Evidence for the charmless annihilation decay mode $B_s^0 \to \pi^+\pi^-$

T. Aaltonen,[21] B. Álvarez González[w],[9] S. Amerio,[41] D. Amidei,[32] A. Anastassov,[36] A. Annovi,[17] J. Antos,[12] G. Apollinari,[15] J.A. Appel,[15] A. Apresyan,[46] T. Arisawa,[56] A. Artikov,[13] J. Asaadi,[51] W. Ashmanskas,[15] B. Auerbach,[59] A. Aurisano,[51] F. Azfar,[40] W. Badgett,[15] A. Barbaro-Galtieri,[26] V.E. Barnes,[46] B.A. Barnett,[23] P. Barria[dd],[44] P. Bartos,[12] M. Bauce[bb],[41] G. Bauer,[30] F. Bedeschi,[44] D. Beecher,[28] S. Behari,[23] G. Bellettini[cc],[44] J. Bellinger,[58] D. Benjamin,[14] A. Beretvas,[15] A. Bhatti,[48] M. Binkley*,[15] D. Bisello[bb],[41] I. Bizjak[hh],[28] K.R. Bland,[5] B. Blumenfeld,[23] A. Bocci,[14] A. Bodek,[47] D. Bortoletto,[46] J. Boudreau,[45] A. Boveia,[11] L. Brigliadori[aa],[6] A. Brisuda,[12] C. Bromberg,[33] E. Brucken,[21] M. Bucciantonio[cc],[44] J. Budagov,[13] H.S. Budd,[47] S. Budd,[22] K. Burkett,[15] G. Busetto[bb],[41] P. Bussey,[19] A. Buzatu,[31] C. Calancha,[29] S. Camarda,[4] M. Campanelli,[28] M. Campbell,[32] F. Canelli[11],[15] B. Carls,[22] D. Carlsmith,[58] R. Carosi,[44] S. Carrillo[k],[16] S. Carron,[15] B. Casal,[9] M. Casarsa,[15] A. Castro[aa],[6] P. Catastini,[20] D. Cauz,[52] V. Cavaliere,[22] M. Cavalli-Sforza,[4] A. Cerri[e],[26] L. Cerrito[q],[28] Y.C. Chen,[1] M. Chertok,[7] G. Chiarelli,[44] G. Chlachidze,[15] F. Chlebana,[15] K. Cho,[25] D. Chokheli,[13] J.P. Chou,[20] W.H. Chung,[58] Y.S. Chung,[47] C.I. Ciobanu,[42] M.A. Ciocci[dd],[44] A. Clark,[18] C. Clarke,[57] G. Compostella[bb],[41] M.E. Convery,[15] J. Conway,[7] M.Corbo,[42] M. Cordelli,[17] C.A. Cox,[7] D.J. Cox,[7] F. Crescioli[cc],[44] C. Cuenca Almenar,[59] J. Cuevas[w],[9] R. Culbertson,[15] D. Dagenhart,[15] N. d'Ascenzo[u],[42] M. Datta,[15] P. de Barbaro,[47] S. De Cecco,[49] G. De Lorenzo,[4] M. Dell'Orso[cc],[44] C. Deluca,[4] L. Demortier,[48] J. Deng[b],[14] M. Deninno,[6] F. Devoto,[21] M. d'Errico[bb],[41] A. Di Canto[cc],[44] B. Di Ruzza,[44] J.R. Dittmann,[5] M. D'Onofrio,[27] S. Donati[cc],[44] P. Dong,[15] M. Dorigo,[52] T. Dorigo,[41] K. Ebina,[56] A. Elagin,[51] A. Eppig,[32] R. Erbacher,[7] D. Errede,[22] S. Errede,[22] N. Ershaidat[z],[42] R. Eusebi,[51] H.C. Fang,[26] S. Farrington,[40] M. Feindt,[24] J.P. Fernandez,[29] C. Ferrazza[ee],[44] R. Field,[16] G. Flanagan[s],[46] R. Forrest,[7] M.J. Frank,[5] M. Franklin,[20] J.C. Freeman,[15] Y. Funakoshi,[56] I. Furic,[16] M. Gallinaro,[48] J. Galyardt,[10] J.E. Garcia,[18] A.F. Garfinkel,[46] P. Garosi[dd],[44] H. Gerberich,[22] E. Gerchtein,[15] S. Giagu[ff],[49] V. Giakoumopoulou,[3] P. Giannetti,[44] K. Gibson,[45] C.M. Ginsburg,[15] N. Giokaris,[3] P. Giromini,[17] M. Giunta,[44] G. Giurgiu,[23] V. Glagolev,[13] D. Glenzinski,[15] M. Gold,[35] D. Goldin,[51] N. Goldschmidt,[16] A. Golossanov,[15] G. Gomez,[9] G. Gomez-Ceballos,[30] M. Goncharov,[30] O. González,[29] I. Gorelov,[35] A.T. Goshaw,[14] K. Goulianos,[48] S. Grinstein,[4] C. Grosso-Pilcher,[11] R.C. Group[55],[15] J. Guimaraes da Costa,[20] Z. Gunay-Unalan,[33] C. Haber,[26] S.R. Hahn,[15] E. Halkiadakis,[50] A. Hamaguchi,[39] J.Y. Han,[47] F. Happacher,[17] K. Hara,[53] D. Hare,[50] M. Hare,[54] R.F. Harr,[57] K. Hatakeyama,[5] C. Hays,[40] M. Heck,[24] J. Heinrich,[43] M. Herndon,[58] S. Hewamanage,[5] D. Hidas,[50] A. Hocker,[15] W. Hopkins[f],[15] D. Horn,[24] S. Hou,[1] R.E. Hughes,[37] M. Hurwitz,[11] U. Husemann,[59] N. Hussain,[31] M. Hussein,[33] J. Huston,[33] G. Introzzi,[44] M. Iori[ff],[49] A. Ivanov[o],[7] E. James,[15] D. Jang,[10] B. Jayatilaka,[14] E.J. Jeon,[25] M.K. Jha,[6] S. Jindariani,[15] W. Johnson,[7] M. Jones,[46] K.K. Joo,[25] S.Y. Jun,[10] T.R. Junk,[15] T. Kamon,[51] P.E. Karchin,[57] A. Kasmi,[5] Y. Kato[n],[39] W. Ketchum,[11] J. Keung,[43] V. Khotilovich,[51] B. Kilminster,[15] D.H. Kim,[25] H.S. Kim,[25] H.W. Kim,[25] J.E. Kim,[25] M.J. Kim,[17] S.B. Kim,[25] S.H. Kim,[53] Y.K. Kim,[11] N. Kimura,[56] M. Kirby,[15] S. Klimenko,[16] K. Kondo*,[56] D.J. Kong,[25] J. Konigsberg,[16] A.V. Kotwal,[14] M. Kreps,[24] J. Kroll,[43] D. Krop,[11] N. Krumnack[l],[5] M. Kruse,[14] V. Krutelyov[c],[51] T. Kuhr,[24] M. Kurata,[53] S. Kwang,[11] A.T. Laasanen,[46] S. Lami,[44] S. Lammel,[15] M. Lancaster,[28] R.L. Lander,[7] K. Lannon[v],[37] A. Lath,[50] G. Latino[cc],[44] T. LeCompte,[2] E. Lee,[51] H.S. Lee,[11] J.S. Lee,[25] S.W. Lee[x],[51] S. Leo[cc],[44] S. Leone,[44] J.D. Lewis,[15] A. Limosani[r],[14] C.-J. Lin,[26] J. Linacre,[40] M. Lindgren,[15] E. Lipeles,[43] A. Lister,[18] D.O. Litvintsev,[15] C. Liu,[45] Q. Liu,[46] T. Liu,[15] S. Lockwitz,[59] A. Loginov,[59] D. Lucchesi[bb],[41] J. Lueck,[24] P. Lujan,[26] P. Lukens,[15] G. Lungu,[48] J. Lys,[26] R. Lysak,[12] R. Madrak,[15] K. Maeshima,[15] K. Makhoul,[30] S. Malik,[48] G. Manca[a],[27] A. Manousakis-Katsikakis,[3] F. Margaroli,[46] C. Marino,[24] M. Martínez,[4] R. Martínez-Ballarín,[29] P. Mastrandrea,[49] M.E. Mattson,[57] P. Mazzanti,[6] K.S. McFarland,[47] P. McIntyre,[51] R. McNulty[i],[27] A. Mehta,[27] P. Mehtala,[21] A. Menzione,[44] C. Mesropian,[48] T. Miao,[15] D. Mietlicki,[32] A. Mitra,[1] H. Miyake,[53] S. Moed,[20] N. Moggi,[6] M.N. Mondragon[k],[15] C.S. Moon,[25] R. Moore,[15] M.J. Morello,[15] J. Morlock,[24] P. Movilla Fernandez,[15] A. Mukherjee,[15] Th. Muller,[24] P. Murat,[15] M. Mussini[aa],[6] J. Nachtman[m],[15] Y. Nagai,[53] J. Naganoma,[56] I. Nakano,[38] A. Napier,[54] J. Nett,[51] C. Neu,[55] M.S. Neubauer,[22] J. Nielsen[d],[26] L. Nodulman,[2] O. Norniella,[22] E. Nurse,[28] L. Oakes,[40] S.H. Oh,[14] Y.D. Oh,[25] I. Oksuzian,[55] T. Okusawa,[39] R. Orava,[21] L. Ortolan,[4] S. Pagan Griso[bb],[41] C. Pagliarone,[52] E. Palencia[e],[9] V. Papadimitriou,[15] A.A. Paramonov,[2] J. Patrick,[15] G. Pauletta[gg],[52] M. Paulini,[10] C. Paus,[30] D.E. Pellett,[7] A. Penzo,[52] T.J. Phillips,[14] G. Piacentino,[44] E. Pianori,[43] J. Pilot,[37] K. Pitts,[22] C. Plager,[8] L. Pondrom,[58] K. Potamianos,[46] O. Poukhov*,[13] F. Prokoshin[y],[13] A. Pronko,[15] F. Ptohos[g],[17] E. Pueschel,[10] G. Punzi[cc],[44] J. Pursley,[58] A. Rahaman,[45] V. Ramakrishnan,[58] N. Ranjan,[46] I. Redondo,[29] P. Renton,[40] M. Rescigno,[49] T. Riddick,[28] F. Rimondi[aa],[6] L. Ristori[44],[15] A. Robson,[19]

T. Rodrigo,[9] T. Rodriguez,[43] E. Rogers,[22] S. Rolli[h],[54] R. Roser,[15] M. Rossi,[52] F. Rubbo,[15] F. Ruffini[dd],[44] A. Ruiz,[9] J. Russ,[10] V. Rusu,[15] A. Safonov,[51] W.K. Sakumoto,[47] Y. Sakurai,[56] L. Santi[gg],[52] L. Sartori,[44] K. Sato,[53] V. Saveliev[u],[42] A. Savoy-Navarro,[42] P. Schlabach,[15] A. Schmidt,[24] E.E. Schmidt,[15] M.P. Schmidt*,[59] M. Schmitt,[36] T. Schwarz,[7] L. Scodellaro,[9] A. Scribano[dd],[44] F. Scuri,[44] A. Sedov,[46] S. Seidel,[35] Y. Seiya,[39] A. Semenov,[13] F. Sforza[cc],[44] A. Sfyrla,[22] S.Z. Shalhout,[7] T. Shears,[27] P.F. Shepard,[45] M. Shimojima[t],[53] S. Shiraishi,[11] M. Shochet,[11] I. Shreyber,[34] A. Simonenko,[13] P. Sinervo,[31] A. Sissakian*,[13] K. Sliwa,[54] J.R. Smith,[7] F.D. Snider,[15] A. Soha,[15] S. Somalwar,[50] V. Sorin,[4] P. Squillacioti,[44] M. Stancari,[15] M. Stanitzki,[59] R. St. Denis,[19] B. Stelzer,[31] O. Stelzer-Chilton,[31] D. Stentz,[36] J. Strologas,[35] G.L. Strycker,[32] Y. Sudo,[53] A. Sukhanov,[16] I. Suslov,[13] K. Takemasa,[53] Y. Takeuchi,[53] J. Tang,[11] M. Tecchio,[32] P.K. Teng,[1] J. Thom[f],[15] J. Thome,[10] G.A. Thompson,[22] E. Thomson,[43] P. Ttito-Guzmán,[29] S. Tkaczyk,[15] D. Toback,[51] S. Tokar,[12] K. Tollefson,[33] T. Tomura,[53] D. Tonelli,[15] S. Torre,[17] D. Torretta,[15] P. Totaro,[41] M. Trovato[ee],[44] Y. Tu,[43] F. Ukegawa,[53] S. Uozumi,[25] A. Varganov,[32] F. Vázquez[k],[16] G. Velev,[15] C. Vellidis,[3] M. Vidal,[29] I. Vila,[9] R. Vilar,[9] J. Vizán,[9] M. Vogel,[35] G. Volpi[cc],[44] P. Wagner,[43] R.L. Wagner,[15] T. Wakisaka,[39] R. Wallny,[8] S.M. Wang,[1] A. Warburton,[31] D. Waters,[28] M. Weinberger,[51] W.C. Wester III,[15] B. Whitehouse,[54] D. Whiteson[b],[43] A.B. Wicklund,[2] E. Wicklund,[15] S. Wilbur,[11] F. Wick,[24] H.H. Williams,[43] J.S. Wilson,[37] P. Wilson,[15] B.L. Winer,[37] P. Wittich[g],[15] S. Wolbers,[15] H. Wolfe,[37] T. Wright,[32] X. Wu,[18] Z. Wu,[5] K. Yamamoto,[39] J. Yamaoka,[14] T. Yang,[15] U.K. Yang[p],[11] Y.C. Yang,[25] W.-M. Yao,[26] G.P. Yeh,[15] K. Yi[m],[15] J. Yoh,[15] K. Yorita,[56] T. Yoshida[j],[39] G.B. Yu,[14] I. Yu,[25] S.S. Yu,[15] J.C. Yun,[15] A. Zanetti,[52] Y. Zeng,[14] and S. Zucchelli[aa6]

(CDF Collaboration[†])

[1]*Institute of Physics, Academia Sinica, Taipei, Taiwan 11529, Republic of China*
[2]*Argonne National Laboratory, Argonne, Illinois 60439, USA*
[3]*University of Athens, 157 71 Athens, Greece*
[4]*Institut de Fisica d'Altes Energies, ICREA, Universitat Autonoma de Barcelona, E-08193, Bellaterra (Barcelona), Spain*
[5]*Baylor University, Waco, Texas 76798, USA*
[6]*Istituto Nazionale di Fisica Nucleare Bologna, [aa] University of Bologna, I-40127 Bologna, Italy*
[7]*University of California, Davis, Davis, California 95616, USA*
[8]*University of California, Los Angeles, Los Angeles, California 90024, USA*
[9]*Instituto de Fisica de Cantabria, CSIC-University of Cantabria, 39005 Santander, Spain*
[10]*Carnegie Mellon University, Pittsburgh, Pennsylvania 15213, USA*
[11]*Enrico Fermi Institute, University of Chicago, Chicago, Illinois 60637, USA*
[12]*Comenius University, 842 48 Bratislava, Slovakia; Institute of Experimental Physics, 040 01 Kosice, Slovakia*
[13]*Joint Institute for Nuclear Research, RU-141980 Dubna, Russia*
[14]*Duke University, Durham, North Carolina 27708, USA*
[15]*Fermi National Accelerator Laboratory, Batavia, Illinois 60510, USA*
[16]*University of Florida, Gainesville, Florida 32611, USA*
[17]*Laboratori Nazionali di Frascati, Istituto Nazionale di Fisica Nucleare, I-00044 Frascati, Italy*
[18]*University of Geneva, CH-1211 Geneva 4, Switzerland*
[19]*Glasgow University, Glasgow G12 8QQ, United Kingdom*
[20]*Harvard University, Cambridge, Massachusetts 02138, USA*
[21]*Division of High Energy Physics, Department of Physics, University of Helsinki and Helsinki Institute of Physics, FIN-00014, Helsinki, Finland*
[22]*University of Illinois, Urbana, Illinois 61801, USA*
[23]*The Johns Hopkins University, Baltimore, Maryland 21218, USA*
[24]*Institut für Experimentelle Kernphysik, Karlsruhe Institute of Technology, D-76131 Karlsruhe, Germany*
[25]*Center for High Energy Physics: Kyungpook National University, Daegu 702-701, Korea; Seoul National University, Seoul 151-742, Korea; Sungkyunkwan University, Suwon 440-746, Korea; Korea Institute of Science and Technology Information, Daejeon 305-806, Korea; Chonnam National University, Gwangju 500-757, Korea; Chonbuk National University, Jeonju 561-756, Korea*
[26]*Ernest Orlando Lawrence Berkeley National Laboratory, Berkeley, California 94720, USA*
[27]*University of Liverpool, Liverpool L69 7ZE, United Kingdom*
[28]*University College London, London WC1E 6BT, United Kingdom*
[29]*Centro de Investigaciones Energeticas Medioambientales y Tecnologicas, E-28040 Madrid, Spain*
[30]*Massachusetts Institute of Technology, Cambridge, Massachusetts 02139, USA*
[31]*Institute of Particle Physics: McGill University, Montréal, Québec, Canada H3A 2T8; Simon Fraser University, Burnaby, British Columbia, Canada V5A 1S6; University of Toronto, Toronto, Ontario, Canada M5S 1A7; and TRIUMF, Vancouver, British Columbia, Canada V6T 2A3*

[32]University of Michigan, Ann Arbor, Michigan 48109, USA
[33]Michigan State University, East Lansing, Michigan 48824, USA
[34]Institution for Theoretical and Experimental Physics, ITEP, Moscow 117259, Russia
[35]University of New Mexico, Albuquerque, New Mexico 87131, USA
[36]Northwestern University, Evanston, Illinois 60208, USA
[37]The Ohio State University, Columbus, Ohio 43210, USA
[38]Okayama University, Okayama 700-8530, Japan
[39]Osaka City University, Osaka 588, Japan
[40]University of Oxford, Oxford OX1 3RH, United Kingdom
[41]Istituto Nazionale di Fisica Nucleare, Sezione di Padova-Trento, [bb]University of Padova, I-35131 Padova, Italy
[42]LPNHE, Universite Pierre et Marie Curie/IN2P3-CNRS, UMR7585, Paris, F-75252 France
[43]University of Pennsylvania, Philadelphia, Pennsylvania 19104, USA
[44]Istituto Nazionale di Fisica Nucleare Pisa, [cc]University of Pisa,
[dd]University of Siena and [ee]Scuola Normale Superiore, I-56127 Pisa, Italy
[45]University of Pittsburgh, Pittsburgh, Pennsylvania 15260, USA
[46]Purdue University, West Lafayette, Indiana 47907, USA
[47]University of Rochester, Rochester, New York 14627, USA
[48]The Rockefeller University, New York, New York 10065, USA
[49]Istituto Nazionale di Fisica Nucleare, Sezione di Roma 1,
[ff]Sapienza Università di Roma, I-00185 Roma, Italy
[50]Rutgers University, Piscataway, New Jersey 08855, USA
[51]Texas A&M University, College Station, Texas 77843, USA
[52]Istituto Nazionale di Fisica Nucleare Trieste/Udine,
I-34100 Trieste, [gg]University of Udine, I-33100 Udine, Italy
[53]University of Tsukuba, Tsukuba, Ibaraki 305, Japan
[54]Tufts University, Medford, Massachusetts 02155, USA
[55]University of Virginia, Charlottesville, Virginia 22906, USA
[56]Waseda University, Tokyo 169, Japan
[57]Wayne State University, Detroit, Michigan 48201, USA
[58]University of Wisconsin, Madison, Wisconsin 53706, USA
[59]Yale University, New Haven, Connecticut 06520, USA

(Dated: August 2, 2011)

We search for new charmless decays of neutral b–mesons to pairs of charged hadrons with the upgraded Collider Detector at the Fermilab Tevatron. Using a data sample corresponding to 6 fb^{-1} of integrated luminosity, we report the first evidence for the $B_s^0 \to \pi^+\pi^-$ decay, with a significance of 3.7σ, and a measured branching ratio $\mathcal{B}(B_s^0 \to \pi^+\pi^-) = (0.57 \pm 0.15\ (\text{stat}) \pm 0.10\ (\text{syst})) \times 10^{-6}$. No evidence is found for the decay $B^0 \to K^+K^-$ and we set a 90% confidence level interval $[0.05, 0.46] \times 10^{-6}$, corresponding to the central value $\mathcal{B}(B^0 \to K^+K^-) = (0.23 \pm 0.10\ (\text{stat}) \pm 0.10\ (\text{syst})) \times 10^{-6}$.

PACS numbers: 13.25.Hw 14.40.Nd

Two-body non-leptonic charmless decays of b–hadrons are widely studied processes in flavor physics. The variety of open channels involving similar final states opens up for investigation an important set of branching fractions and CP asymmetries, allowing a deeper understanding of strong interaction dynamics with the potential to refine the modelling of these processes by effective theories. Some decays receive contributions from higher-order ('penguin') transitions, and are therefore sensitive to the possible presence of new physics in internal loops.

The $B_s^0 \to \pi^+\pi^-$ and $B^0 \to K^+K^-$ decay modes have a special status, in that all quarks in the final state are different from those in the initial state. This limits the possible diagrams that contribute to these decay to penguin-annihilation (PA) and W-exchange (E) topologies (see Fig. 1). These amplitudes are difficult to predict within the current phenomenological models, and are often neglected in calculations. Estimates of these amplitudes in the QCD factorization (QCDF) ap-

*Deceased
[†]With visitors from [a]Istituto Nazionale di Fisica Nucleare, Sezione di Cagliari, 09042 Monserrato (Cagliari), Italy, [b]University of CA Irvine, Irvine, CA 92697, USA, [c]University of CA Santa Barbara, Santa Barbara, CA 93106, USA, [d]University of CA Santa Cruz, Santa Cruz, CA 95064, USA, [e]CERN,CH-1211 Geneva, Switzerland, [f]Cornell University, Ithaca, NY 14853, USA, [g]University of Cyprus, Nicosia CY-1678, Cyprus, [h]Office of Science, U.S. Department of Energy, Washington, DC 20585, USA, [i]University College Dublin, Dublin 4, Ireland, [j]University of Fukui, Fukui City, Fukui Prefecture, Japan 910-0017, [k]Universidad Iberoamericana, Mexico D.F., Mexico, [l]Iowa State University, Ames, IA 50011, USA, [m]University of Iowa, Iowa City, IA 52242, USA, [n]Kinki University, Higashi-Osaka City, Japan 577-8502, [o]Kansas State University, Manhattan, KS 66506, USA, [p]University of Manchester, Manchester M13 9PL, United Kingdom, [q]Queen Mary, University of London, London, E1 4NS, United Kingdom, [r]University of Melbourne, Victoria 3010, Australia, [s]Muons, Inc., Batavia, IL 60510, USA, [t]Nagasaki Institute of Applied Science, Nagasaki, Japan, [u]National Research Nuclear University, Moscow, Russia, [v]University of Notre Dame, Notre Dame, IN 46556, USA, [w]Universidad de Oviedo, E-33007 Oviedo, Spain, [x]Texas Tech University, Lubbock, TX 79609, USA, [y]Universidad Tecnica Federico Santa Maria, 110v Valparaiso, Chile, [z]Yarmouk University, Irbid 211-63, Jordan, [hh]On leave from J. Stefan Institute, Ljubljana, Slovenia,

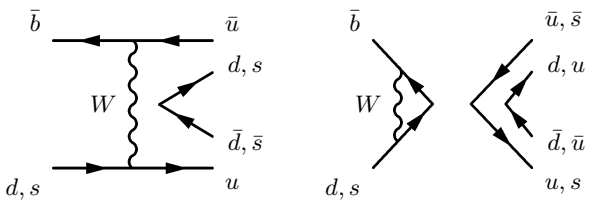

FIG. 1: W-exchange (E, left panel) and penguin-annihilation (PA, right panel) diagrams contributing to $B^0 \to K^+K^-$ and $B_s^0 \to \pi^+\pi^-$ decays.

proach [1, 2] are affected by significant uncertainties. The soft collinear effective theory (SCET) approach provides no estimates at all. Recent perturbative QCD calculations (pQCD) provide some potentially testable predictions [3, 4]. These diagrams can carry different CP-violating and CP-conserving phases with respect to leading diagrams; the lack of knowledge of their size therefore introduces uncertainties in predictions for other well-studied decays, such as $B^0 \to \pi^+\pi^-$ [5, 6].

Up to now, the $B_s^0 \to \pi^+\pi^-$ and $B^0 \to K^+K^-$ decay modes have not been observed, the best upper limits coming from [7, 8]. A measurement of branching fractions of these modes would be particularly useful, since it would allow a better determination of the strength of PA and E amplitudes, due to cancellation of some uncertainties [6].

In this Letter we report the results of a simultaneous search for the two decays $B_s^0 \to \pi^+\pi^-$ and $B^0 \to K^+K^-$ [9], using 6 fb^{-1} of data collected by the upgraded Collider Detector (CDF II) at the Fermilab Tevatron at $\sqrt{s} = 1.96$ TeV.

CDF II is a multipurpose magnetic spectrometer surrounded by calorimeters and muon detectors. The detector components relevant for this analysis are briefly outlined below; a more detailed description can be found in Ref. [10]. A silicon microstrip vertex detector (SVX) and a cylindrical drift chamber (COT) immersed in a 1.4 T axial magnetic field allow reconstruction of charged–particle trajectories (tracks) in the pseudorapidity range $|\eta| < 1.0$ [11]. The SVX consists of five concentric layers of double-sided silicon sensors with radii between 2.5 and 22 cm, each providing a measurement with up to 15 (70) μm resolution in the ϕ (z) direction. The COT has 96 measurement layers, between 40 and 137 cm in radius, organized into alternating axial and $\pm 2^\circ$ stereo superlayers. The transverse momentum resolution is $\sigma_{p_T}/p_T^2 \sim 0.15\%/(\mathrm{GeV}/c)$, corresponding to a typical mass resolution of 22 MeV/c^2 for our signals. The specific ionization energy loss (dE/dx) of charged particles in the COT can be measured from the collected charge, which is logarithmically encoded in the output pulse width of each wire, and provides 1.4σ separation between kaons and pions with momenta greater than 2 GeV/c.

The data were collected by a three-level trigger system, using a set of requirements specifically aimed at selecting two-pronged B decays. At level 1, COT tracks are reconstructed in the transverse plane by a hardware processor (XFT). Two opposite-charge particles are required, with reconstructed transverse momenta $p_{T1}, p_{T2} > 2$ GeV/c, the scalar sum $p_{T1} + p_{T2} > 5.5$ GeV/c, and an azimuthal opening-angle $\Delta\phi < 135^\circ$. At level 2, the silicon vertex trigger (SVT) combines XFT tracks with SVX hits to measure the impact parameter d (distance of closest approach to the beam line) of each track with 45 μm resolution. The requirement of two tracks with $0.1 < d < 1.0$ mm reduces the background from light quark processes by two orders of magnitude while preserving about half of the signal. A tighter opening-angle requirement, $20^\circ < \Delta\phi < 135^\circ$, preferentially selects two–body B decays over multi–body decays with 97% efficiency and further reduces background. Each track pair is then used to form a B candidate, which is required to have an impact parameter $d_B < 140$ μm and to have traveled, before decaying, a distance $L_T > 200$ μm in the transverse plane. At level 3, an array of computers confirms the selection with a full event reconstruction. The overall acceptance of the trigger selection is $\approx 2\%$ for b–hadrons with $p_T > 4$ GeV/c and $|\eta| < 1$.

The offline selection is based on a more accurate determination of the same quantities used in the trigger, with the addition of two further observables: the isolation (I_B) of the B candidate [12], and the quality of the three-dimensional fit (χ^2 with 1 d.o.f.) of the decay vertex of the B candidate. Requiring a large value of I_B further reduces the background from light-quark jets, and a low χ^2 reduces the background from decays of different long-lived particles that may exist in the event, owing to the good resolution of the SVX detector in the z direction. We use the same final selection originally devised for the $B_s^0 \to K^-\pi^+$ search [8], whose simulation has proven to be nearly optimal also for detection of $B_s^0 \to \pi^+\pi^-$. This includes the following criteria: $I_B > 0.525$, $\chi^2 < 5$, $d > 120$ μm, $d_B < 60$ μm, and $L_T > 350$ μm.

No more than one B candidate per event is found after this selection, and a mass ($m_{\pi\pi}$) is assigned to each, using a charged pion mass assignment for both decay products. The resulting mass distribution is shown in Fig. 2, and is dominated by the overlapping contributions of the $B^0 \to K^+\pi^-$, $B^0 \to \pi^+\pi^-$, and $B_s^0 \to K^+K^-$ modes [13, 14], with backgrounds coming from mis-reconstructed multi-body b–hadron decays (physics background) and random pairs of charged particles (combinatorial background). A $B^0 \to K^+K^-$ signal would appear in this distribution as an enhancement around 5.18 GeV/c^2, while a $B_s^0 \to \pi^+\pi^-$ signal is expected at the nominal B_s^0 mass of 5.3663 GeV/c^2, where other, more abundant modes, contribute [8].

We used an extended unbinned likelihood fit, incorporating kinematic (kin) and particle identification (PID) information, to determine the fraction of each individual

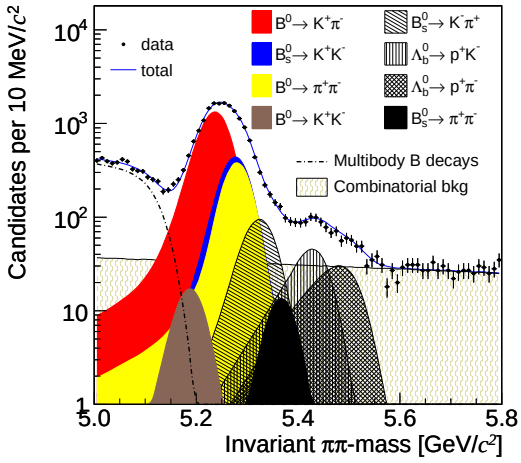

FIG. 2: Mass distribution of reconstructed candidates. The charged pion mass is assigned to both tracks. The sum of the fitted distributions and the individual components of signal and background are overlaid on the data distribution.

mode in our sample. The likelihood is defined as

$$\mathcal{L} = \frac{\nu^N}{N!} e^{-\nu} \cdot \prod_{i=1}^{N} \mathcal{L}_i \qquad (1)$$

where N is the total number of observed candidates, ν is the estimator of N to be determined by the fit, and the likelihood for the ith event is

$$\begin{aligned} \mathcal{L}_i &= (1-b)\sum_j f_j \mathcal{L}_j^{\rm kin}\mathcal{L}_j^{\rm PID} \\ &+ b\left(f_{\rm p}\mathcal{L}_{\rm p}^{\rm kin}\mathcal{L}_{\rm p}^{\rm PID} + (1-f_{\rm p})\mathcal{L}_{\rm c}^{\rm kin}\mathcal{L}_{\rm c}^{\rm PID}\right), \end{aligned} \qquad (2)$$

where the index j runs over all signal modes, and the index 'p' ('c') labels the physics (combinatorial) background terms. The f_j are the signal fractions to be determined by the fit, together with the background fraction parameters b and $f_{\rm p}$.

For each charged hadron pair, the kinematic information is summarized by three loosely correlated observables: (a) the squared mass $m^2_{\pi\pi}$; (b) the charged momentum asymmetry $\beta = (p_+ - p_-)/(p_+ + p_-)$, where p_+ (p_-) is the momentum of the positive(negative) particle; (c) the scalar sum of particle momenta $p_{tot} = p_+ + p_-$. The above variables allow evaluation of the squared invariant mass m^2_{+-} of a candidate for any mass assignment of the positive and negative decay products (m_+,m_-), using the equation

$$\begin{aligned} m^2_{+-} &= m^2_{\pi\pi} - 2m^2_\pi + m^2_+ + m^2_- + \\ &-2\sqrt{p^2_+ + m^2_\pi}\sqrt{p^2_- + m^2_\pi} + 2\sqrt{p^2_+ + m^2_+}\sqrt{p^2_- + m^2_-}, \end{aligned} \qquad (3)$$

where $p_+ = p_{tot}\frac{1+\beta}{2}$, $p_- = p_{tot}\frac{1-\beta}{2}$.

The kinematic distributions of the physics signal are obtained from Monte Carlo simulations, while the combinatorial background distributions are extracted from real data [15]. The squared mass distribution of the combinatorial background is parameterized by an exponential function. The slope is fixed in the fit to the value extracted from an enriched sample of two generic random tracks, containing events passing all requirements of final selections except for vertex quality, replaced by an anti-selection cut $\chi^2 > 40$, which strongly rejects track pairs originating from a common vertex.

The background from partially reconstructed decays of generic B hadrons is modeled by an ARGUS function [16] convoluted with a Gaussian resolution. The parameters of the ARGUS function are free to vary in the fit. To ensure the reliability of the search for small signals in the vicinity of larger peaks, the shapes of the mass distributions assigned to each signal have been modeled in detail. Momentum dependence and non–Gaussian resolution tails are accounted for by a full simulation of the detector, while the effects of soft photon radiation in the final state are simulated by PHOTOS [17]. This resolution model was accurately checked against the observed shape of the 3.2×10^6 $D^0 \to K^-\pi^+$ and 140×10^3 $D^0 \to \pi^+\pi^-$ signals in a sample of $D^{*+} \to D^0\pi^+$ decays, collected with a similar trigger selection.

The $D^{*+} \to D^0\pi^+$ sample was also used to calibrate the dE/dx response of the drift chamber to kaons and pions, using the charge of the D^{*+} pion to identify the D^0 decay products. The dE/dx response of protons was determined from a sample of about 167,000 $\Lambda \to p\pi^-$ decays, where the kinematics and the momentum threshold of the trigger allow unambiguous identification of the decay products [18]. PID information is summarized by a single observable kaonness $\kappa_{+(-)}$ for positive (negative) track, defined as:

$$\kappa_{+(-)} = \frac{dE/dx_{+(-)} - dE/dx_{+(-)}(\pi)}{dE/dx_{+(-)}(K) - dE/dx_{+(-)}(\pi)} \qquad (4)$$

where $dE/dx_{+(-)}(\pi)$ and $dE/dx_{+(-)}(K)$ are the expected $dE/dx_{+(-)}$ depositions for those particle assignments. Statistical separation between kaons and pions is about 1.4σ, while the ionization rates of protons and kaons is quite similar in the momentum range of the decay products. The physics background model allows for independent, charge-averaged contributions of pions and kaons, whose fractions are determined by the fit. The combinatorial background model allows for independent contributions of positively and negatively charged pions and kaons, whose fractions are determined by the fit. Muons are indistinguishable from pions with the available dE/dx resolution and are therefore incorporated into the pion component. For similar reasons, the small proton component has been incorporated within the kaon component.

TABLE I: Yields and significances of rare mode signals. The first quoted uncertainty is statistical, the second is systematic.

Mode	N_s	Significance
$B^0 \to K^+K^-$	$120 \pm 49 \pm 42$	2.0σ
$B_s^0 \to \pi^+\pi^-$	$94 \pm 28 \pm 11$	3.7σ

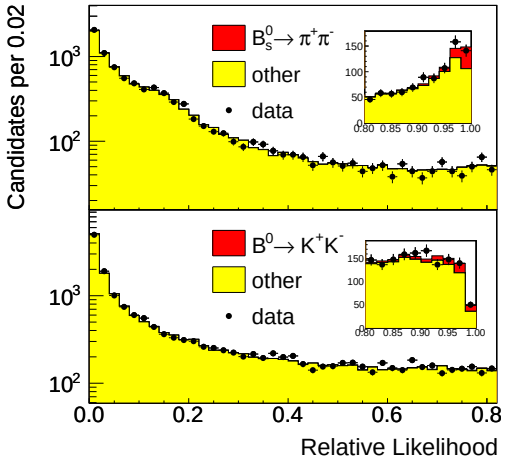

FIG. 3: Distribution of the relative signal likelihood, $\mathcal{L}_S/(\mathcal{L}_S + \mathcal{L}_{\rm other})$, in the region $5.25 < m_{\pi\pi} < 5.50$ GeV/c^2 for $B_s^0 \to \pi^+\pi^-$ and $5.10 < m_{\pi\pi} < 5.35$ GeV/c^2 for $B^0 \to K^+K^-$. For each event, $\mathcal{L}_S$ is the likelihood for the $B_s^0 \to \pi^+\pi^-$ (top panel) and $B^0 \to K^+K^-$ (bottom panel) signal hypotheses, and $\mathcal{L}_{\rm other}$ is the likelihood for everything but the chosen signal, i.e. the weighted combination of all other components according to their measured fractions. Points with error bars show the distributions of data and histograms show the distributions predicted from the measured fractions.

From the signal fractions returned by the fit we calculate the signal yields shown in Table I. The significance of each signal is evaluated as the ratio of the yield observed in data to its total uncertainty (statistical and systematic), as determined from a simulation where the size of that signal is set to zero. This evaluation assumes a Gaussian distribution of yield estimates, supported by the results obtained from repeated fits to simulated samples. This procedure yields a more accurate measure of significance with respect to the purely statistical estimate obtained from $\sqrt{-2\Delta\ln(\mathcal{L})}$.

We obtain a significant signal for the $B_s^0 \to \pi^+\pi^-$ mode (3.7σ), while no evidence is found for the $B^0 \to K^+K^-$ mode (2.0σ). Figure 3 shows relative likelihood distributions for these modes, which are in good agreement with our model.

To avoid large uncertainties associated with production cross sections and absolute reconstruction efficiency, we measure all branching fractions relative to the $B^0 \to K^+\pi^-$ mode. A frequentist limit [19] at the 90% C.L. is quoted for the $B^0 \to K^+K^-$ mode. The raw fractions returned by the fit are corrected for the differences in selection efficiencies between different modes, which do not exceed 10%. These corrections are determined from detailed detector simulation, with only two exceptions that are measured from data: the momentum-averaged relative isolation efficiency between B_s^0 and B^0, and the difference in efficiency for triggering on kaons and pions due to the different specific ionization in the COT. The former is determined as 1.00 ± 0.03 from fully-reconstructed samples of $B_s^0 \to J/\psi\phi$, and $B^0 \to J/\psi K^{*0}$ decays [18]. Only b–hadrons decaying into pairs of charged hadrons are simulated and no fragmentation products, collision remnants, or pile-up events are present. The latter is determined from samples of D^0 mesons decaying into pairs of charged hadrons [15]. We measure the relative branching fractions $\mathcal{B}(D^0 \to \pi^+\pi^-)/\mathcal{B}(D^0 \to K^-\pi^+)$ and $\mathcal{B}(D^0 \to K^+K^-)/\mathcal{B}(D^0 \to K^-\pi^+)$. The numbers of events are extracted from the available samples of tagged $D^0 \to \pi^+\pi^-$, $D^0 \to K^-\pi^+$ and $D^0 \to K^+K^-$ decays, fitting the invariant $D^*\pi$ mass spectrum [15], while reconstruction efficiencies are determined from the same simulation used for the measurements described in this Letter. Comparison of these numbers with world measurement averages [20] allows us to extract the correction needed to compensate for the different efficiency of the tracking trigger for kaons and pions. The final corrections applied to our result do not exceed 5% and are independent of particle momentum.

The dominant contribution to the systematic uncertainty on the $B_s^0 \to \pi^+\pi^-$ branching fraction is due to the dE/dx model, which derives from the statistical uncertainty on the 48 parameters used for the analytical description of the correlated dE/dx response of the two decay products [18]. This uncertainty is evaluated by repeating the likelihood fit 200 times with different sets of those parameters, randomly extracted from a multi-dimensional sphere, centered in the central value of the parameterization, with a radius corresponding to 1σ of statistical uncertainty, neglecting their correlation. The dE/dx-induced systematic uncertainty on each observable is then obtained as the standard deviation of the distribution of that observable, over the ensemble of likelihood fits performed with different sets of parameters. This approach is adequate for our purposes since the present measurement is statistically dominated.

Further uncertainties have been assessed, due to the physics background model and the uncertainty on the relative efficiency corrections. The time evolution of the $B_s^0 \to \pi^+\pi^-$ mode is potentially different from the flavor-

TABLE II: Measured relative branching fractions of rare modes. Absolute branching fractions were derived by normalizing to the current world–average value $\mathcal{B}(B^0 \to K^+\pi^-) = (19.4 \pm 0.6) \times 10^{-6}$, and assuming the average values at high energy for the production fractions: $f_s/f_d = 0.282 \pm 0.038$ [20]. The first quoted uncertainty is statistical, the second is systematic.

Mode	Relative $\mathcal{B}$	Absolute $\mathcal{B}$ (10^{-6})	Limit (10^{-6})
$B^0 \to K^+K^-$	$\frac{\mathcal{B}(B^0\to K^-K^+)}{\mathcal{B}(B^0\to K^+\pi^-)} = 0.012 \pm 0.005 \pm 0.005$	$0.23 \pm 0.10 \pm 0.10$	$[0.05, 0.46]$ at 90% C.L.
$B_s^0 \to \pi^+\pi^-$	$\frac{f_s}{f_d}\frac{\mathcal{B}(B_s^0\to \pi^-\pi^+)}{\mathcal{B}(B^0\to K^+\pi^-)} = 0.008 \pm 0.002 \pm 0.001$	$0.57 \pm 0.15 \pm 0.10$	–

specific modes if the width difference $\Delta\Gamma_s$ between the B_s^0 mass eigenstates is significant, due to its containing a superposition of the flavor eigenstates of the B_s^0 meson. This may affect the efficiency of the event selection relative to the normalization mode $B^0 \to K^+\pi^-$. We derive our result under the assumption that the $B_s^0 \to \pi^+\pi^-$ mode is dominated by the short-lived B_s^0 component, that $\Gamma_s = \Gamma_d$, and $\Delta\Gamma_s/\Gamma_s = 0.92^{+0.051}_{-0.054}$ [20]. This introduces a small uncertainty which is accounted for in the final quoted systematic uncertainty. A further systematic uncertainty of the order of 10%, is included for the $B^0 \to K^+K^-$ mode to account for a small bias of the fitting procedure observed in simulated samples. Other contributions come from trigger efficiencies, physics background shape, kinematics, b–hadron masses and lifetimes, and transverse momentum distribution of the Λ_b^0 baryon.

The final results are listed in Table II. Absolute branching fractions are also quoted, by normalizing to world-average values of production fractions and $\mathcal{B}(B^0 \to K^+\pi^-)$ [20]. The branching fraction measured for the $B_s^0 \to \pi^+\pi^-$ mode is consistent with the previous upper limit ($< 1.2 \times 10^{-6}$ at 90% C.L.), based on a subsample of the current data [8]. It agrees with predictions obtained with the pQCD approach [3, 4], but it is higher than most other theoretical predictions [1, 2, 21].

The measurement of $\mathcal{B}(B^0 \to K^+K^-)$ is the world's best and supersedes the previous limit [13]. The central value is in agreement with other existing measurements [20] and with theoretical predictions [1, 2].

In summary, we have searched for new rare charmless decay modes of neutral b–mesons into pairs of charged mesons in CDF data. We report an updated upper limit for the $B^0 \to K^+K^-$ mode, the first evidence for the $B_s^0 \to \pi^+\pi^-$ mode and a measurement of its branching fraction.

We thank the Fermilab staff and the technical staffs of the participating institutions for their vital contributions. This work was supported by the U.S. Department of Energy and National Science Foundation; the Italian Istituto Nazionale di Fisica Nucleare; the Ministry of Education, Culture, Sports, Science and Technology of Japan; the Natural Sciences and Engineering Research Council of Canada; the National Science Council of the Republic of China; the Swiss National Science Foundation; the A.P. Sloan Foundation; the Bundesministerium für Bildung und Forschung, Germany; the Korean World Class University Program, the National Research Foundation of Korea; the Science and Technology Facilities Council and the Royal Society, UK; the Institut National de Physique Nucleaire et Physique des Particules/CNRS; the Russian Foundation for Basic Research; the Ministerio de Ciencia e Innovación, and Programa Consolider-Ingenio 2010, Spain; the Slovak R&D Agency; and the Academy of Finland.

[1] M. Beneke and M. Neubert, Nucl. Phys. **B675**, 333 (2003).
[2] H.-Y. Cheng, and C.-K. Chua, Phys. Rev. D **80**, 114026 (2009); Phys. Rev. D **80**, 114008 (2009).
[3] A. Ali *et al.*, Phys. Rev. D **76**, 074018 (2007).
[4] Y. Li, C.-D. Lu, Z.-J. Xiao, and X.-Q. Yu, Phys. Rev. D **70**, 034009 (2004).
[5] A. Soni and D. A. Suprun, Phys. Rev. D **75**, 054006 (2007).
[6] A. J. Buras, R. Fleischer, S. Recksiegel, and F. Schwab, Nucl. Phys. **B697**, 133 (2004).
[7] B. Aubert *et al.* (*BABAR* Collaboration), Phys. Rev. D **75**, 012008 (2007); K. Abe *et al.* (Belle Collaboration), Phys. Rev. Lett. **98**, 181804 (2007).
[8] A. Aaltonen *et al.* (CDF Collaboration), Phys. Rev. Lett. **103**, 031801 (2009).
[9] Throughout this paper, C-conjugate modes are implied and branching fractions indicate CP-averages.
[10] D. Acosta *et al.* (CDF Collaboration), Phys. Rev. D **71**, 032001 (2005); A. Sill (CDF Collaboration), Nucl. Instrum. Methods A **447**, 1 (2000); A. Affolder *et al.*, Nucl. Instrum. Methods A **453**, 84 (2000); T. Affolder *et al.*, Nucl. Instrum. Methods A **526**, 249 (2004).
[11] CDF II uses a cylindrical coordinate system in which ϕ is the azimuthal angle, r is the radius from the nominal beam line, and z points in the proton beam direction, with the origin at the center of the detector. The transverse plane is the plane perpendicular to the z axis.
[12] Isolation is defined as $I_B = p_T(B)/(p_T(B) + \sum_i p_{Ti})$, where $p_T(B)$ is the transverse momentum of the B candidate, and the sum runs over all other tracks within a cone of radius 1, in η-ϕ space around the B flight-direction.
[13] A. Abulencia *et al.* (CDF Collaboration), Phys. Rev. Lett. **97**, 211802 (2006).
[14] A. Aaltonen *et al.* (CDF Collaboration), Phys. Rev. Lett. **106**, 181802 (2011).
[15] F. Ruffini, Ph.D. Thesis, Università di Siena, Siena, in preparation.
[16] Defined as $m^2_{\pi\pi} \cdot \sqrt{1-(m^2_{\pi\pi}/m^2_{\rm A})^2} \cdot e^{-c_{\rm A}\cdot(m^2_{\pi\pi}/m^2_{\rm A})^2}$ if $m^2_{\pi\pi} < m^2_{\rm A}$. The cutoff $m^2_{\rm A}$ is fixed while the coefficient $c_{\rm A}$ is a free parameter in out fit. See H. Albrecht *et al.*

(ARGUS Collaboration), Phys. Lett. B **241**, 278 (1990).
[17] E. Barberio and Z. Was, Comput. Phys. Commun. **79**, 291 (1994).
[18] M.J. Morello, Ph.D. Thesis, Scuola Normale Superiore, Pisa, Fermilab Report No. FERMILAB-THESIS-2007-57 (2007).
[19] G. J. Feldman and R. D. Cousins, Phys. Rev. D **57**, 3873 (1998).
[20] K. Nakamura *et al.*, J. Phys. G **37**, 075021 (2010).
[21] J.-F. Sun, G.-H. Zhu, and D.-S. Du, Phys. Rev. D **68**, 054003 (2003).